Path following controller for autonomous vehicles

Conference Paper · November 2019

DOI: 10.1109/ICCVE45908.2019.8964960

2 authors:

Ádám Domina
Budapest University of Technology and Economics
4 PUBLICATIONS **5** CITATIONS
SEE PROFILE

Viktor Tihanyi
Budapest Unviersity of Technology and Ecnomics
28 PUBLICATIONS **54** CITATIONS
SEE PROFILE

Path following controller for autonomous vehicles

Ádám Domina
Department of Automotive Technologies
Budapest University of Technology and Economics
Budapest, Hungary
adam.domina@gjt.bme.hu

Viktor Tihanyi
Department of Automotive Technologies
Budapest University of Technology and Economics
Budapest, Hungary
viktor.tihanyi@gjt.bme.hu

***Abstract* — In recent years vehicles with high level of automation are becoming more popular which is expected to continue in the future. Advanced driving assistance systems are increasingly taking control of the vehicle, starting with the support of the driving task. Automated or highly automated vehicles are expected to follow a planned road safely. In this paper, the authors aim to improve the accuracy of path following by developing a new control strategy. The controller includes both pure pursuit and Stanley methods, the operation of the controller is based on the geometry of the vehicle and the path; the key is the proper weighting between two controllers. The performance of the combined path following controller was measured on a demonstration vehicle.**

Keywords—autonomous vehicle, path following, controller, Stanley, pure pursuit, combined controller, lateral dynamic vehicle model

I. INTRODUCTION

In recent years the developers in vehicle industry mostly focused on autonomous vehicles. In the future this trend is expected to continue and strengthen. The reason of this trend is to make the road transport environmentally friendly, more efficient, safer and faster. The testing and validation methods of these autonomous systems are still under development [1].

Four layers form the architecture of an autonomous vehicle: the driver interface layer, the environmental perception layer [2], the command layer and the executive layer. The subject of this article is the lateral motion control of the vehicle which is located in the executive layer.

Fig. 1. Smart demonstration vehicle

In previous articles of the authors [13], a weighting method was developed combining the command of the pure pursuit and the Stanley controllers with various weights. The weighting is the function of the geometry of the vehicle and the path. This method was tested in simulation environment. In this article the results of this method tested on a demonstration vehicle will be presented.

A. Simulation and real test environment

The developed features are first tested in a software environment which is easy to verify, safe and if the used vehicle model correctly fits the real vehicle, it gives corresponding results. When the simulation shows acceptable results, the controller can be tested on the real vehicle in a sealed, secure place. The simulations were done in Matlab and Simulink software.

B. Smart demonstration vehicle

The Department of Automotive Technologies owns a demonstration vehicle which is a Smart Fortwo shown in Fig. 1. The vehicle is equipped with an Autobox as a central computer, a dual, high precision GNSS system with RTK correction to ensure redundancy, an intelligent camera, a RADAR and LIDARs. If one of the GNSS systems does not work properly, the other can replace it which is essential for accurate and safe path following. The demonstration vehicle is able to realize valet parking, traffic jam assist and platooning functions. The vehicle is suitable for testing the combined controller algorithm.

In this article firstly the used vehicle model is introduced in section 2. Secondly, the principle of the pure pursuit and the Stanley controllers, as well as the combined controller with weighting method is explained in section 3. Finally, the simulation results are presented in section 4.

II. VEHICLE MODEL

The used vehicle model is the widely used lateral dynamic bicycle model. The model contains the lateral dynamics of the vehicle and is expanded with an equation which describes the dynamics of steering. This additional equation published by the authors [3] is based on measurements on the demonstration vehicle. Assuming constant speed, the longitudinal dynamics of the car is neglected. This reduces the computational cost and has negligible effect on the simulation results.

Equation (1) and (2) describe the motion of the vehicle [4], equation (3) describes the dynamics of the steering system. This additional equation allows the simulation to model the time delay of the steering which is essential for accurate modelling of the different motion forms, for example the oscillation.

$$\dot{v}_y = \frac{-c_f\left[tan^{-1}\left(\frac{v_y + l_f\omega}{v_x}\right) - \delta\right]cos(\delta) - c_r\, tan^{-1}\left(\frac{v_y - l_r\omega}{v_x}\right)}{m} - v_x\omega \quad (1)$$

$$\dot{\omega} = \frac{-l_f c_f\left[tan^{-1}\left(\frac{v_y + l_f\omega}{v_x}\right) - \delta\right]cos(\delta) + l_r c_r\, tan^{-1}\left(\frac{v_y - l_r\omega}{v_x}\right)}{I_z} \quad (2)$$

$$M_{mot} = M_{tire} * i_{cw} + M_{sa} * i_{cw} + \Theta * \ddot{\delta} \quad (3)$$

In (1) and (2) v_y is the lateral, v_x is the longitudinal speed of the vehicle, c_f and c_r are the cornering stiffness of the front and the rear tires, ω is the yaw-rate of the vehicle, δ is the steering angle, m is the mass of the vehicle, I_z is the inertia of the vehicle around the z-axis, l_f and l_r are the distance between the centre of the gravity and the front and rear axles. In (3) M_{mot} is the total torque generated by the electric steering servo motor, and M_{tire} is the steering resistant torque of the tire, around the z-axis of the tire, which is the result of the frictional contact between the tire and the road surface. M_{sa} is the self-aligning moment of the wheel generated by the pneumatic trail of the tire, i_{cw} is the wheel-column transmission ratio in the steering system, and Θ is the inertia of the steering system, reduced to the steering column, including the column, pinion, hub, rack and wheels, and lastly $\ddot{\delta}$ is the angular acceleration of the steering column. M_{tire} and M_{sa} determined with measurements are the function of vehicle speed and axle load [5], [6] which are either calculated or read from lookup tables during the simulation.

III. Path Following Controllers

In this section firstly the pure pursuit and the Stanley path following controllers are presented, then the weighting method is demonstrated which describes the weighting between the commands of the controllers.

A. Pure pursuit controller

The pure pursuit is a commonly used controller which has several advantages: easy to implement, works robustly, has low computational cost and grants appropriate path following performance.

The principle of the controller is to fit a semi-circle through the rear wheel of the vehicle and a reference point in the path [7]. The rear wheel of the bicycle model is at the half of the gauge of the real vehicle, at the rear axle. The reference point is measured with an L distance before the vehicle which distance is called lookahead. The semi-circle is tangent to the heading direction of the vehicle at the rear wheel. Equation (4) describes the steering command of the controller, where W is the wheelbase of the vehicle, R is the turning radius, α is the angle between the vehicle heading and the line between the rear wheel and the target point of the lookahead on the path.

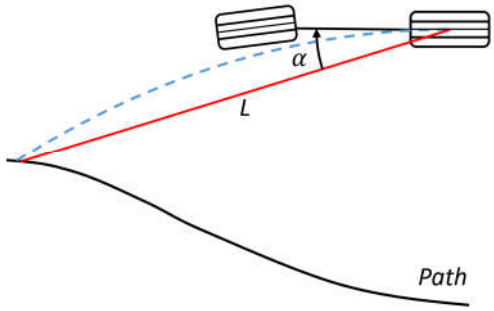

Fig. 2. Pure pursuit geometry

$$\delta = tan^{-1}\left(\frac{W}{R}\right) = tan^{-1}\left(\frac{2Wsin(\alpha)}{L}\right) \quad (4)$$

This controller is liable to cut the corners, especially if the lookahead is large, but the operation is stable and is not liable to overshoot at the corners [8]. The cutting effect is caused by the lookahead because the controller always looks forward and does not consider the current distance between the vehicle and the path. When the lookahead distance is small, the vehicle tends to follow the track more accurately, but an oscillation will occur, hence, the average lateral error will increase. If the lookahead is large, the vehicle will converge to the path slower, but the cutting corner effect will increase. The right choice of the lookahead is a good compromise for mitigating errors.

B. Stanley controller

The Stanley method is based on two errors with respect to the path. The orientation and the distance error are both calculated at the closest path point [9]. The Stanley geometry is shown on Fig. 3.

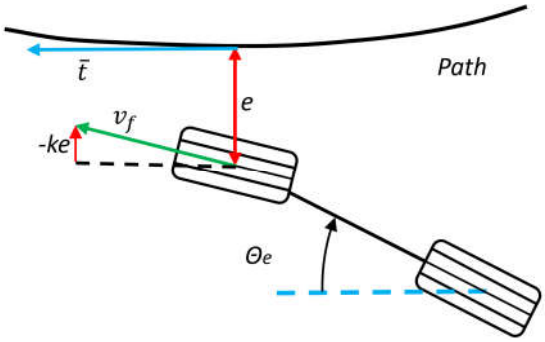

Fig. 3. Stanley geometry

The Stanley controller gives a lateral velocity to the vehicle using the steering angle. The desired lateral velocity is the function of the errors. Equation (5) describes the steering command of the Stanley controller.

$$\delta = tan^{-1}\left(-ke/v_f\right) - \Theta_e \quad (5)$$

In (5) k is the tuning parameter of the controller, e is the lateral error at the nearest point, v_f is the longitudinal velocity of the vehicle and Θ_e is the orientation error.

If the value of k is large, the vehicle converges to the path fast, but is liable to oscillate along the path. If k is small, the vehicle converges slower, but the oscillation is negligible. If the curvature of the path is not changing continuously, the controller gives a large lateral error which occurs due to the lack of any lookahead strategy, hence the vehicle starts the steering at the corner. On smooth path the controller grants accurate and safe path following.

C. Combined Controller and Weighting Method

As shown above, both controllers have their own advantages and disadvantages. Pure pursuit is comprehensively good but cutting corners, while Stanley significantly overshoots at corners but is good at smooth paths. A hybrid controller in [10] was presented to combine the advantages of the two controllers. Also In [10], the weighting of the command of the two controllers depends on the smoothness of the path. The object of this article is to

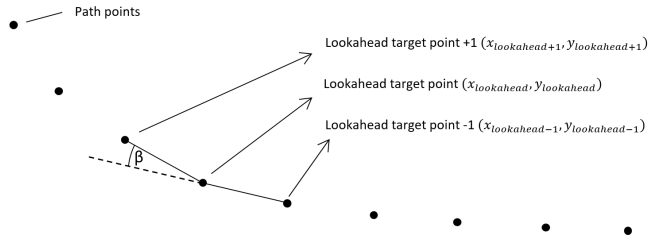

Fig. 4. Calculation of path smoothness

develop a new weighting method and test it on a real vehicle. The weighting method is based on the geometry of the path and the vehicle. The weighting method considers the minimum turn radius that can be realized by the vehicle. On a track with a smaller radius the vehicle is unable to pass without significant lateral error due to the geometric characteristics of the vehicle.

The path is characterized by the smoothness which is calculated with the same method than in [10], described by (6), shown in Fig. 4.

$$\beta = tan^{-1}\left(\frac{y_{lookahead+1} - y_{lookahead}}{x_{lookahead+1} - x_{lookahead}}\right) - tan^{-1}\left(\frac{y_{lookahead} - y_{lookahead-1}}{x_{lookahead} - x_{lookahead-1}}\right) \quad (6)$$

Given the distance between the path points and given the turning circle, the maximum achievable β value can be determined. The distance d between the path points is assumed to be constant along the entire path - in this case 0.5 meter. The geometry is shown in Fig. 5. The maximal value of β is calculated by (7).

$$\beta_{max} = 2 * \left(sin^{-1}\frac{d/2}{R}\right) \quad (7)$$

In (7) R is the radius of the turning circle. The minimum turning radius of the vehicle is known, the diameter of the turning circle of the Smart demonstration vehicle is 7 meter so the radius is 3.5 meter. If the path contains sections where $\beta > \beta_{max}$, the vehicle can follow the path but a large lateral error will occur. The value of β is always calculated in the current target point of the lookahead. The constant lookahead is set to 2 meter. The lookahead is weighted with the speed i.e. as the speed increases, the lookahead increases (8) by multiplying the speed with a weight factor k_l which has been optimized, taking the optimal value 0.4.

$$L = 2 + k_l * v \quad (8)$$

The k gain value of the Stanley controller in (5) also has been optimized, taking the optimal value 1.9. The parameter of k_l and k was optimized in simulation, the lateral error values was calculated with different values, the parameters with the smallest error have selected.

Knowing β_{max} and the current value of β is the base of the weighting between the commands of the two controllers. If β=0, the weight of Stanley is 80%, while the weight of pure pursuit is 20%. If $\beta >= \beta_{max}$, then the weight of Stanley is 20% and the weight of pure pursuit is 80%. Between these limits the weight of pure pursuit is linearly increasing as the value of β is increasing, described by (9). The value of β saturates if the path contains sections where β is greater than β_{max}. The algorithm considers β as β_{max}.

$$k_{pp} = k_{min} + \frac{\beta}{\beta_{max}}(k_{max} - k_{min}) \quad (9)$$

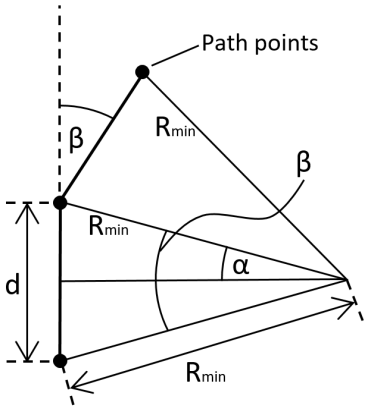

Fig. 5. Geometry of path points and smoothness

In (9) k_{min}=0.2 as 20%, k_{max}=0.8 as 80 %, k_{pp} is the weight of the command of pure pursuit controller. The weight of Stanley, k_{st} is calculated in (10).

$$k_{st} = 1 - k_{pp} \quad (10)$$

The final, weighted steering angle δ command is given by (11).

$$\delta = k_{pp} * \delta_{pp} + k_{st} * \delta_{st} \quad (11)$$

In (11) δ_{pp} is the steering angle command of pure pursuit controller, and δ_{st} is the steering angle command of Stanley controller.

D. Reference path for testing

The performance of the controllers are needed to be tested on a real vehicle. For this purpose a reference path was recorded with the GNSS system of the vehicle. The reference path is shown in Fig. 6. There are two representative sections on the path: an s-curve and a reversing curve. At these sections the overshoot and oscillation phenomena, and other lateral errors are well observable.

The reference path contains straight sections and curves. These curves have different curvatures. Driving along this versatile trajectory, the performance of the controllers are comparable.

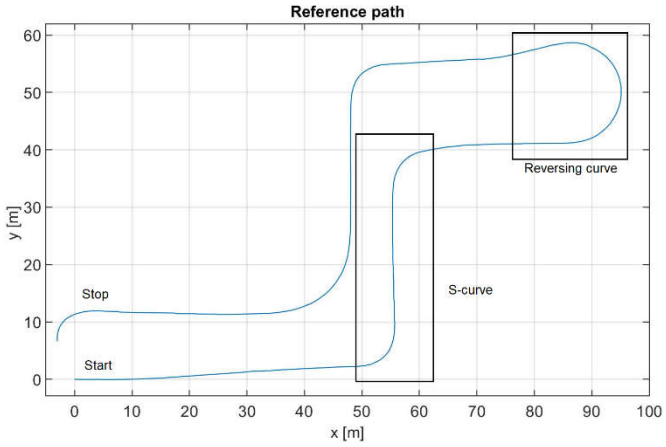

Fig. 6. Reference path

IV. Measurement resutls

There were nine tests ran at 10 km/h, 15 km/h and 20 km/h, with all three controllers. The measurement results are shown in Fig. 7, Fig. 8 and Fig. 9. Two types of defective form of movement are distinguished: the overshoot and the oscillation. The oscillation is also referred to in the literature as chattering effect [12]. As the speed increased, the Stanley controller started to oscillate along the path, especially during cornering manoeuvres. At low speed the results show comprehensively good performance; there was no overshoot or oscillation, the lateral error was small. According to the figures there was no significant difference between the controllers. As speed increased, the error also increased. At the straight sections the oscillation appeared. The pure pursuit showed the least oscillation, while the Stanley showed the most. The figures clearly show that the sign of the combined controller is a mixture of the other two. The combined controller shows less overshoot at the corners than Stanley, and at the straight sections converges faster to the path after the corners. The oscillation appeared by pure pursuit, too, but it was not as significant as Stanley. At straight sections the command of combined controller is 80% made of Stanley command hence the combined controller shows oscillation that was effectively decreased by the 20% weight of pure pursuit.

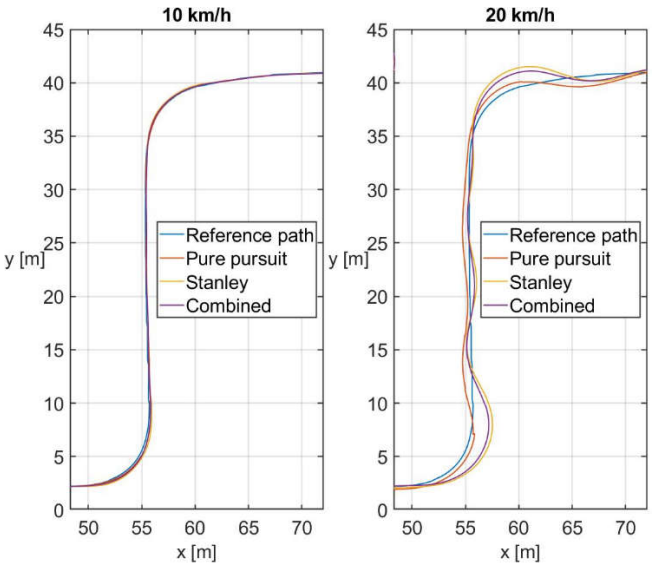

Fig. 7. Test results at S-curve, at 10 km/h and 20 km/h

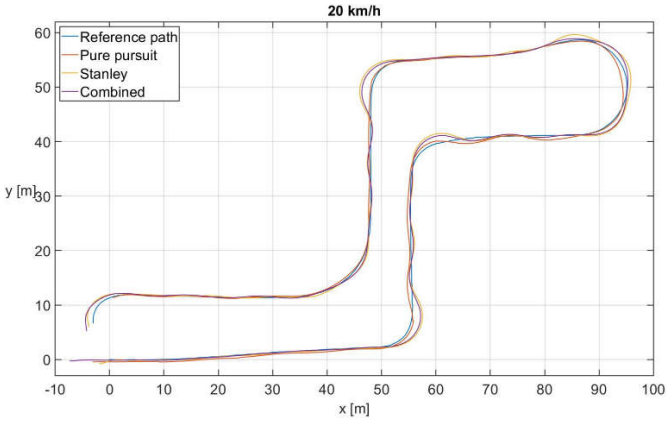

Fig. 8. Test results on the reference path at 20 km/h

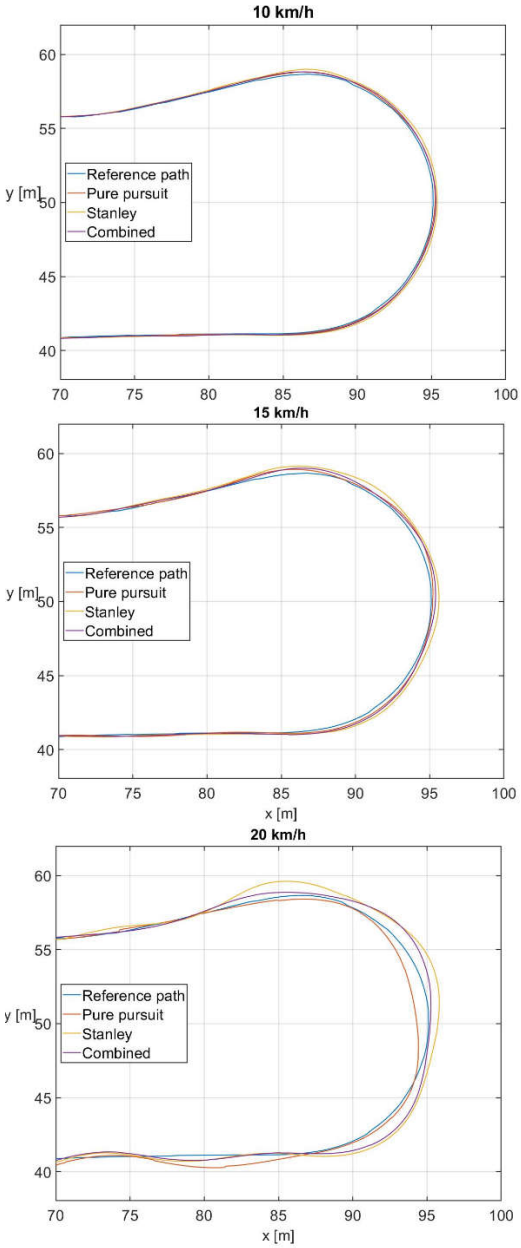

Fig. 9. Test results at reversing curve, with different speed

TABLE I. Lateral Error Values

Speed	Lateral error: average [m] / maximum [m]		
	Pure pursuit	*Stanley*	*Combined*
10 km/h	0.0702 / 0.4253	0.1132 / 0.3560	0.079 / 0.2272
15 km/h	0.1081 / 0.7513	0.1942 / 1.0477	0.1259 / 0.6352
20 km/h	0.2917 / 0.9641	0.3938 / 2.1972	0.2923 / 1.7953

After performing the measurements it is necessary to quantify the lateral error. There are several indicators for the tracking error in [11], while in this article the cross tracking error was calculated. The calculated errors are shown in Table I. The results show how the lateral error increases with increasing speed. Generally the pure pursuit controller gives the smallest error, the Stanley gives the largest. Based on the measurement results, the Stanley controller is too sensitive for the lateral error which is responsible for the oscillation. This can be theoretically improved by reducing the k parameter of

the controller. During measurements the reduction of the k parameter had no effect on the oscillation hence the measurements were done with the optimized value shown above. Increasing the value of k led to the increasing of the oscillation.

At lower speed the combined controller had the smallest maximal error, the average error of it was close to pure pursuit. As the speed increased, the error of combined controller also increased, but only passing the pure pursuit to a negligible extent. The overshoot and the oscillation were successfully reduced. Based on the results the combined controller provides as accurate path following as the pure pursuit controller, but effectively combines the advantages of the two controllers.

CONCLUSION

In this paper a weighting method is proposed that combines the advantages of pure pursuit and Stanley controllers. The method is based on the smoothness of the path and the minimal turning radius which is feasible by the vehicle. The controllers and the weighting method were implemented, using the optimized k factors of the controllers. Then the controllers were tested in a real vehicle at different speeds. Finally, the lateral error was calculated for every controller. The results show that the combined controller is able to incorporate the advantages of the controllers; the vehicle followed the path more accurately in both curves and straight sections.

ACKNOWLEDGMENT

The project has been supported by the European Union, cofinanced by the European Social Fund. EFOP-3.6.2-16-2017-00002.

REFERENCES

[1] M. Zöldy, “Legal Barriers of Utilization of Autonomous Vehicles as Part of Green Mobility”, Proceedings of the 4th International Congress of Automotive and Transport Engineering (AMMA 2018), 2018

[2] H. Lengyel, Zs. Szalay, „The Significance and Effect of the Traffic System Signaling to the Environment, Present and Future Traffic”, Proceedings of the 4th International Congress of Automotive and Transport Engineering, pp. 847-856, January 2019

[3] Á. Domina, V. Tihanyi, “Modelling the dynamic behavior of the steering system for low speed autonomous path tracking,” 30th IEEE Intelligent Vehicles Symposium, 2019

[4] J. M. Snider, Automatic Steering Methods for Autonomous Automobile Path Tracking. Pittsburg, Pennsylvania: Carnegie Mellon University, 2009

[5] Reza N. Jazar, *Vehicle Dynamics Theory and Application*. Springer, 2008.

[6] G. Rill, *Vehicle Dynamics*. Fachhochschule Regensburg, University of Applied Sciences, August 2007

[7] B. Paden, M. Cap, S. Z. Yong, D. Yershov, and E. Frazzoli, “A survey of motion planning and control techniques for self-driving urban vehicles”, IEEE Transactions on Intelligent Vehicles, vol. 1, pp. 33-55, June 2016

[8] Á. Domina, V. Tihanyi, "Comparison of path following controllers for autonomous vehicles", SAMI 2019 IEEE 17th World Symposium on Applied Machine Intelligence and Informatics, 2019.

[9] N. H. Amer, K. Hudha, H. Zamzuri, V. R. Aparow, A. F. Z. Abidin, Z. A. Kadir, M. Murrad, “Adaptive Trajectory Tracking Controller for an Armoured Vehicle: Hardware-in-the-loop Simulation,” 2018 57th Annual Conference of the Society of Intrument and Control Engineers of Japan (SICE), Nara, Japan, 2018.

[10] M. Cibooglu, U. Karapinar, M. T. Söylemez, “Hybrid Controller Approach for an Autonomous Vehicle Path Trackig Problem”, 25th Mediterranean Conference on Control and Automation (MED) Valletta, Malta, 2017.

[11] N. H. Amer, H. Zamzuri, K. Hudha, Z. A. Kadir, “Modelling and Control Strategies in Path Tracking Control for Autonomous Ground Vehicles: A Review of State of the Art and Challenges ” Journal of Intelligent and Robotic Systems, Springer, 2017, pp 225-254.

[12] A. Pedro Aguiar, Joao P. Hespanha, “Trajectory-Tracking and Path-Following of Underactuated Autonomous Vehicles With Parametric Modeling Uncertainty,” in Transactions on Automatic Control, vol. 52, no. 8, pp. 1362-1379, August 2007.

[13] Á. Domina, V. Tihanyi, “Combined path following controller for autonomous vehicles,” in Perners Contacts, Special Issiue, Vol. 19, pp. 77-84, May 2019